CHAPTER II
LITERATURE REVIEW

2.1 Titanium(IV) oxide

Titanium(IV) oxide is generally known as titanium dioxide or titania, appearing as white solid. Its chemical formula is TiO_2. Due to its brightness and high refractive index (n=2.7), titania is extensively used as a white pigment, providing whiteness and opacity to products, such as paints, plastics, papers, inks, cosmetics and toothpastes. It is also used in sunscreen product due to its high ultraviolet light absorptivity. Fujishima *et al.* (1972) reported potential of titanium dioxide as photocatalyst. Recently, Kasuga (2006) informed utilizing modified titania nanotube in bone regeneration material and proton conduction electrolytic film.

2.1.1 Polymorphs

The general occurrence of titanium(IV) oxide in nature is well-known in three forms (rutile, anatase and brookite). The polymorphs of titania reported to date include rutile, anatase, brookite, TiO_2-B (bronze), TiO_2-R (ramsdellite), TiO_2-H (hollandite), TiO_2-II (columbite), and TiO_2-III (baddeleyite). Details of this distinctive polymorph are listed in table 2.1 (Yang *et al.*, 2009).

Crystalline structure of titania is simply represented as octahedron which titanium atom surrounded by oxygen atom located at the apical sites. Each polymorph of titania has its own arrangement of the octahedrals (Bokhimi *et al.*, 2001). Below, the crystalline structures of rutile and anatase are presented (Figure 2.1).

Table 2.1 Structural parameters of TiO_2 polymorphs

Structure	Space group	Density (g cm^{-3})	Crystal System	Unit cell (Å)
Rutile	$P4_2/mnm$	4.13	Tetragianl	a= 4.59, c= 2.96
Anatase	$I4_1/amd$	3.79	Tetragonal	a= 3.79,c = 9.51
Brookite	Pbca	3.99	Orthorhombic	a= 9.17, b= 5.46, c=5.14
TiO_2 (B)	C2/m	3.64	Monoclinic	a= 12.17, b= 3.74, c= 6.51, β= 107.29°
TiO_2 -II	Pbcn	4.33	Orthorhombic	a = 4.52, b = 5.5, c = 4.94
TiO_2 (H)	I4/m	3.46	Tetragonal	a = 10.18, c = 2.97
TiO_2 - III	$P2_1/c$	4.72	monoclinic	a = 4.64, b = 4.76, c = 4.81, β = 99.2°
TiO_2 (R)	Pbnm	3.87	Orthorhombic	a = 4.9, b = 9.46, c = 2.96

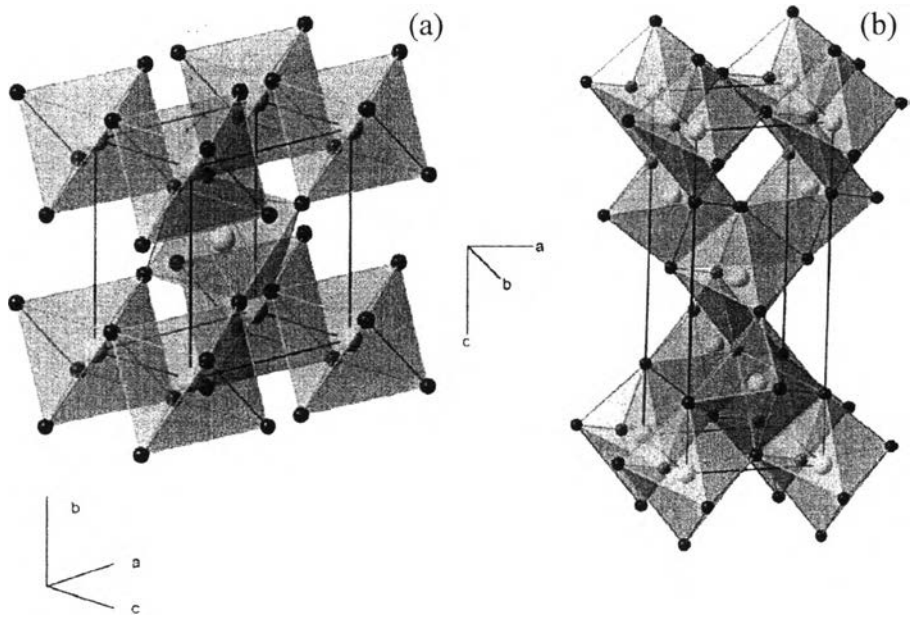

Figure 2.1 Crystalline structures of rutile (a) and anatase (b) (Yang *et al.*, 2009).

2.1.2 Nanotube Structure

TiO_2-based nanotubes have attracted wide attention from research communities. Because, the nanotubes have high specific surface area, ion-changeable ability, and photocatalytic ability, nanotube TiO_2 is suited for development in extensive applications. Currently developed methods of preparing titania nanotubes comprise of assisted–template method (Hoyer, 1996), sol–gel process (Kasuga *et al.*, 1998), electrochemical anodic oxidation (Gong *et al.*, 2001), and hydrothermal treatment (Kasuga *et al.*, 1999).

In the template–assisted method, anodic aluminumoxide (AAO) nanoporous membrane is usually used as template (Figure 2.2). The membrane composes of an array of parallel straight nanopores with uniform diameter and length. The size of nanotubes can be controlled by applied templates. However, the template–assisted method has several difficulties of pre-fabrication and post-removal of the templates which usually results in impurities.

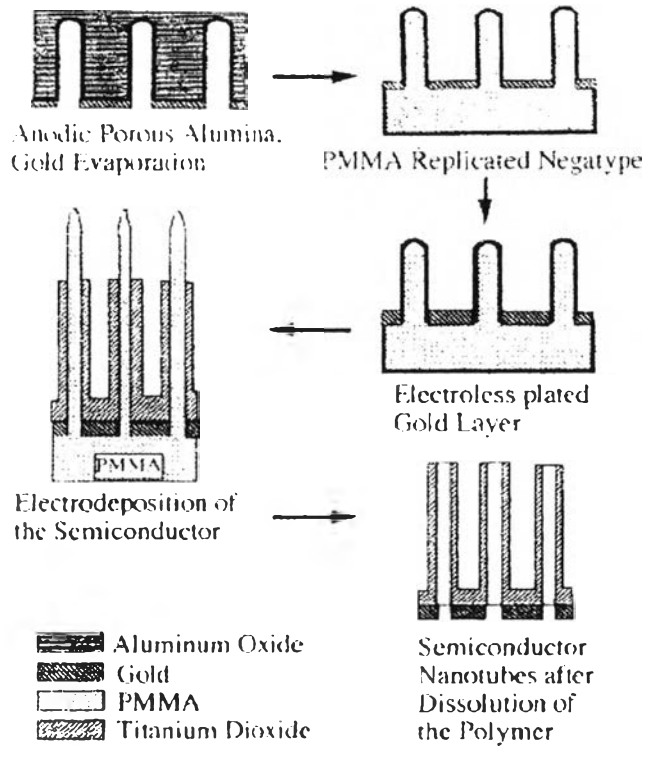

Figure 2.2 Schematic view of template-asisted synthesis pathway (different materials are marked) (Hoyer, 1996).

Regarding the electrochemical anodic oxidation, Gong *et al.* (2001) reported the self-assembled titania nanotubes with highly ordered arrays (Figure 2.3). This method is based on the anodization of Ti foil, obtaining a film of nanoporous titanium oxide (Mor *et al.*, 2006). Mor and co-workers also reported the reviews associated with the fabrication factors, characterizations, formation mechanism, and the analogous applications of titania nanotubes arrays.

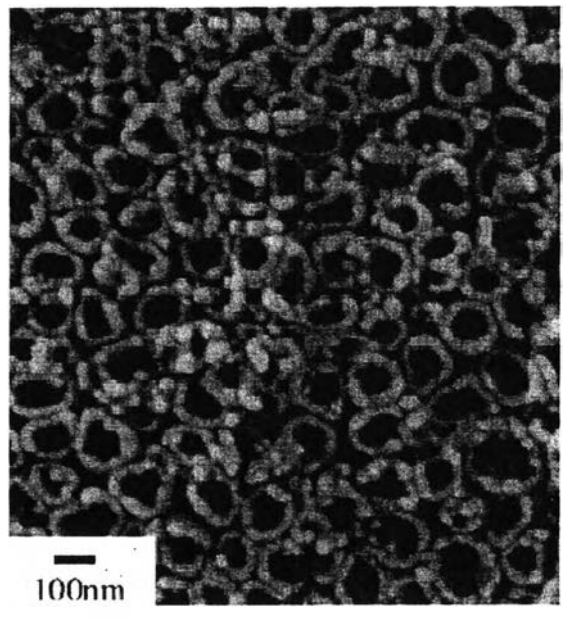

Figure 2.3 FE-SEM top-view image of titania nanotubes synthesized by anodic oxidation method (Gong *et al.*, 2001).

The hydrothermal process is either suitable for large scale production or able to yield very low dimensional, well separated, crystallized nanotubes (Poudel *et al.*, 2005). Titania nanotubes produced by the hydrothermal treatment show good crystallinity and gave a pure-phase structure in one step in a tightly closed vessel.

As above mentioned approaches, the electrochemical anodic oxidation and the hydrothermal treatment have been received wide attention among others, due to their cost-effective, easy procedure, and the feasibility/availability of widespread applications.

A report by Ou *et al.* (2007), showing the chemical strucrure of TNTs, was still under debated, as presented in Table 2.2. According to this review, Ou *et al.*

also mentioned that the formation of $Na_xH_{2-x}Ti_3O_7$ and $Na_xH_{2-x}Ti_2O_4(OH)$ was more acceptable than others.

Table 2.2 Proposed chemical structures of TNTs, crystal systems and lattice parameters

Chemical structure	Crystal system	Lattice parameters
Anatase TiO_2	Tetragonal	a = 3.79 nm, b = 3.79, c = 2.38
$N_2Ti_3O_7$, $Na_2Ti_3O_7$, $Na_xH_{2-x}Ti_3O_7$	Monoclinic	a = 1.926 nm, b = 0.378, c = 0.300, β = 101.45°
$H_2Ti_2O_4(OH)_2$, $Na_2Ti_2O_4(OH)_2$	Orthorhombic	a = 1.808 nm, b = 0.379, c = 0.299
$H_xTi_{2-x/4}\square_{x/4}O_4(H_2O)$	Orthorhombic	a = 0.378 nm, b = 1.874, c = 0.298
$H_2Ti_4O_9(H_2O)$	Monoclinic	a = 1.877 nm, b = 0.375, c = 1.162, β = 104.6°

2.1.2.1 *$Na_xH_{2-x}Ti_3O_7$ Group*

The formation mechanism of $H_2Ti_3O_7$ nanotubes was reported in two pathways. The first one mentioned by Chen et al. (2002) indicated that the nanotubes were constructed by trititanate $(Ti_3O_7)^{2-}$ sheets. The excessive Na^+ intercalation between crystals space allowing trititanate layers exfoliated from the nanocrystal curling to form nanotubes structure. For the other, Chen *et al.* (2002) explained the lack of hydrogen on $(Ti_3O_7)^{2-}$ surface, peeling its plate off the crystals. Chen *et al.* also mentioned that the nanotubes structure was formed by wrapping a (100) plane along AA' (Figure 2.4 (b)). The displacement of A' gave the space between layers at 0.78 nm (Figure 2.4 (c). The structure and cross-section of TNTs were shown in Figure 2.4 (a) and (d), respectively.

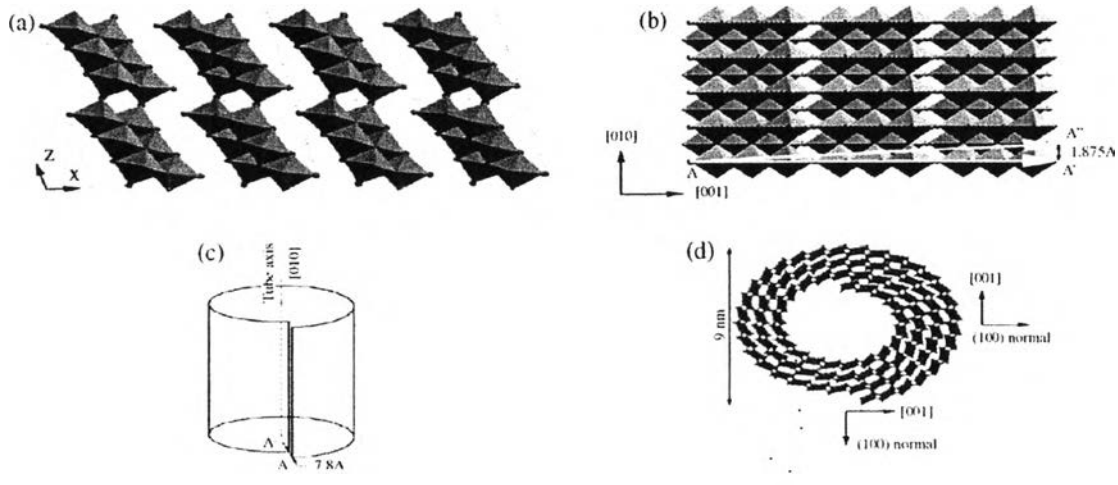

Figure 2.4 The schematics of (a) 2×2 unit cells of $H_2Ti_3O_7$ on the [010] projection, (b) layers of $H_2Ti_3O_7$ along the (100) plane where the nanotube is formed (AA' and AA'' indicate the chiral vectors), (c) the displacement vector of AA' forming a nanotube, and (d) the cross-section structure of TNTs (Ou *et al.*, 2007).

2.1.2.1 *$Na_xH_{2-x}Ti_2O_4(OH)_2$ Group*

The formation mechanism was reported by Yang *et al.* (2003). Starting from the swelling of TiO_2 particles, the nanotube structure was then formed from swelling stripes and peel-off granules. Resulting from the swelling, the short Ti-O bonds in TiO_6 were expected to split under concentrated NaOH solution, resulting in the linear fragment linking each other by O^--Na^+-O^- bonds and forming a flexible planar (Figure 2.5 (a)). Finally, the formation of nanotube structure occurred through the covalent bonding of end groups. The acid washing process produced the ion-exchange of Na^+ by H^+, peeling of individual layers from TiO_2 particles.

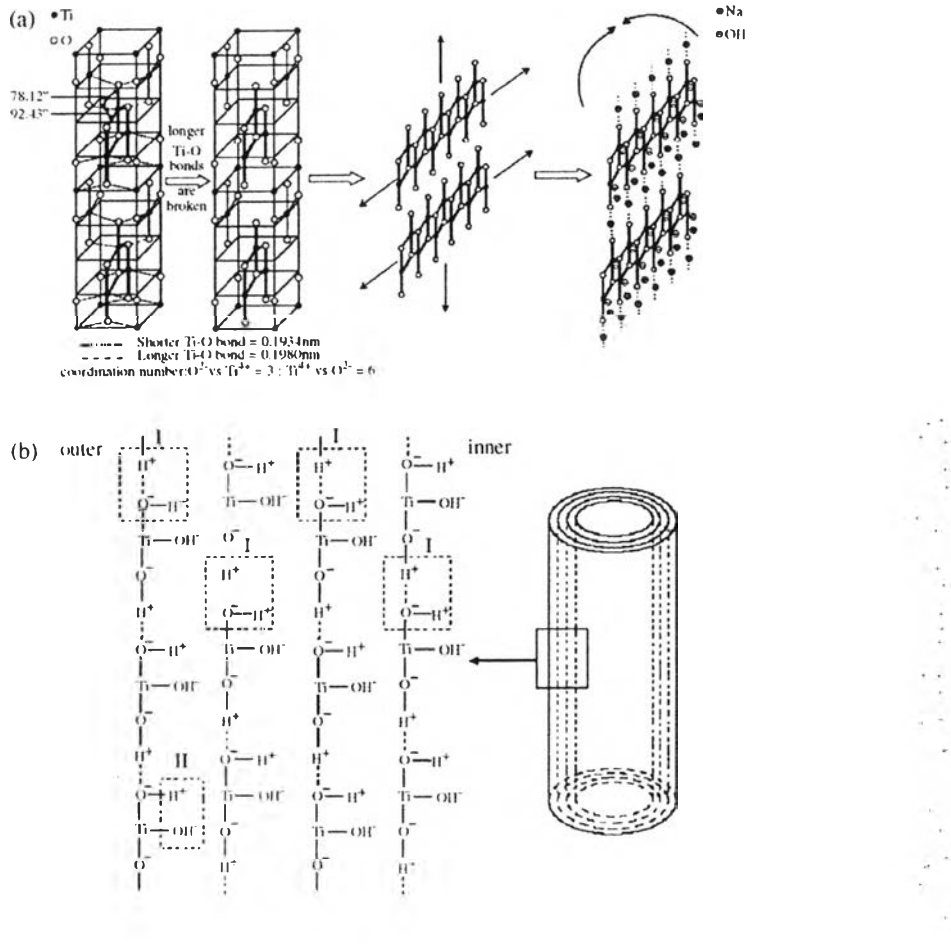

Figure 2.5 The schematic showing the formation of a $Na_2Ti_2O_4(OH)_2$ sheet (a) and the structure of TNTs after acid washing (b) (Ou *et al.*, 2007).

2.2 Microwave Irradiation Hydrothermal Synthesis

The hydrothermal term, originated from two greek words 'hydros' meaning water and 'thermos' meaning heat, was defined in chemistry as any heterogeneous chemical reaction in the presence of a solvent above the room temperature and at pressure greater than 1 atm in a closed system (Byrappa and Adschiri, 2007). The synthesis occurred in an autoclave containing highly corrosive solvent. The autoclave must be operable under high temperature and pressure. The advantages for utilizing hydrothermal synthesis were high product purity and homogeneity, narrow particle size distribution, faster reaction time, lower synthesis temperature, simple equipment, and single-step processes (Byrappa and Adschiri, 2007).

The microwave heating was applied to provide the unique advantage of microwave irradiation which is the direct energy delivering to materials through molecular-level interactions with the impinging electromagnetic field, resulting in uniform, rapid, and volumetric heating (Figure 2.6). The high reaction rates and selectivity are also obtained, thus, reducing the reaction time and giving high product yields (Wu *et al.*, 2005).

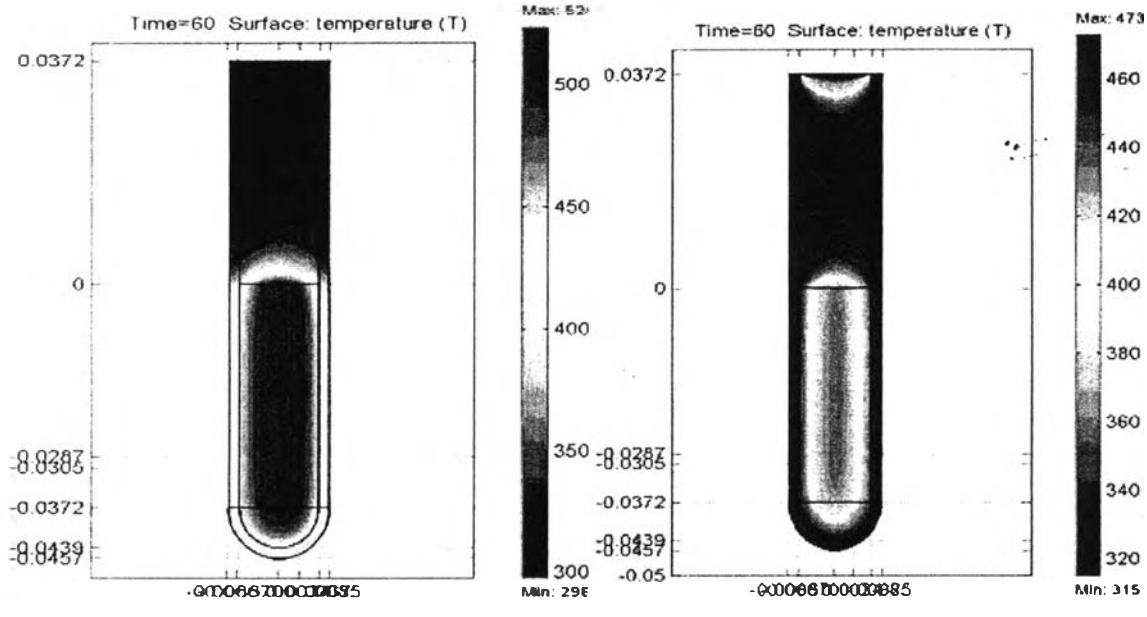

Figure 2.6 The temperature gradient of microwave heating comparing with conventional heating. (biotage.com: April 2011).

2.3 Semiconductor Photocatalyst

According to a review (carp et al., 2004), Semiconductor photocatalyst is an oxidation process to destroy organic pollutants in water. The process system consists of a UV-A light and a semiconductor photocatalyst, such as TiO_2. Titania, categorized as n-type semiconductor and reacted with light having a wavelength less than 390 nm, produces electrons-holes pairs. Electrons were excited and moved from valence band to conduction band. These electrons and holes can initiate oxidation and

reduction reactions. In aqueous systems, holes can react with OH^- to produce OH radical. Whereas the electrons were trapped at surface defect and reacted with O_2 to produce super oxide anion radical. The super oxides further react with H_2O to produce more OH radicals. The hydroxyl radicals will react with the organic pollutants, resulting in mineralization, as shown below (san *et al.*, 2002).

$$TiO_2 + h\nu \rightarrow e^-_{cb} + h^+_{vb}$$

$$H_2O + h^+_{vb} \rightarrow \bullet OH + H^+$$

$$OH^- + h^+_{vb} \rightarrow \bullet OH$$

$$O_2 + e^-_{cb} \rightarrow \bullet O2^-$$

$$\bullet O_2^- + H_2O \rightarrow OH^- + \bullet HO_2$$

$$\bullet HO_2 + \bullet HO_2 \rightarrow H_2O_2 + O_2$$

$$H_2O_2 + \bullet O_2^- \rightarrow \bullet OH + OH^- + O_2$$

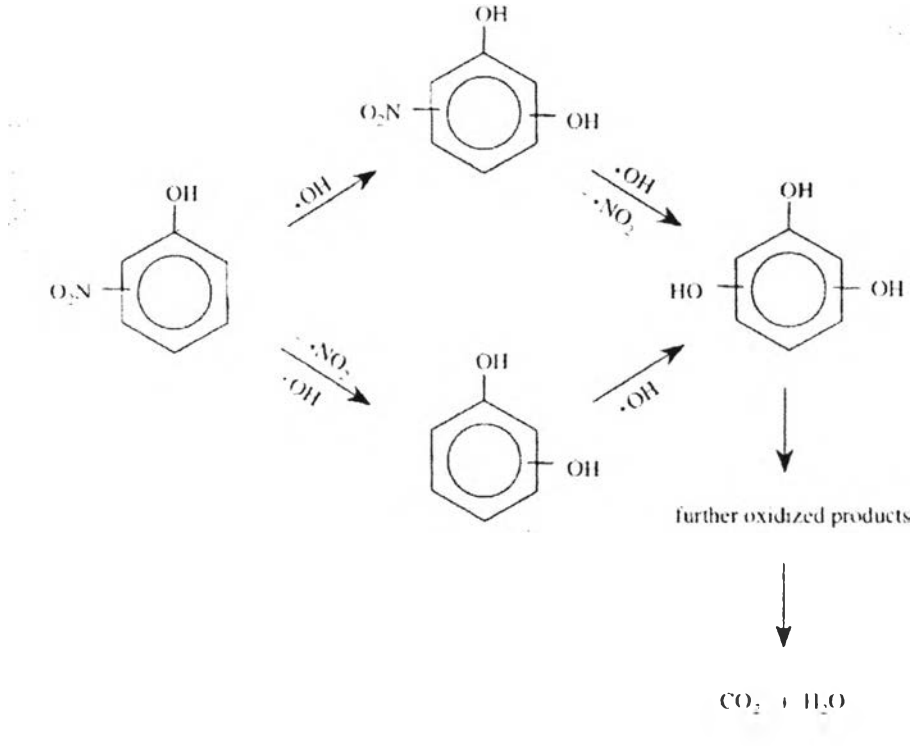

Figure 2.7 The schematic diagram showing photocatalyst degradation mechanism of 4-nitrophenol (paola *et al.*, 2003).